Chapter 16

Quantification of the Elastic Properties of Soft and Sticky Materials Using AFM

Nicolas Bouchonville and Alice Nicolas

Abstract

Indentation Type-AFM (IT-AFM) is very useful to analyze the local rheological properties of soft or biological materials. However, analysis of the force-indentation curves is very sensitive to the way the curves are fitted: fits with elastic models such as Hertz or Sneddon's models performed on parts of the curve that indeed correspond to nonlinear elastic regimes, or that result from significant adhesive interactions of the AFM tip with the material lead to results that can be as much as twice larger than fits performed with appropriate models (nonlinear or adhesive).

Here, we propose a methodology to address rigidity measurements by fitting parts of the force-indentation curves that correspond to the linear elastic response of the material, even in the presence of adhesion. The major contribution of this methodology is to set up an easy-handling criterion to mark out the linear elastic response to indentation, valid either for purely elastic and elasto-adhesive models.

Key words AFM, Mechanics, Rigidity, Elasticity, Adhesion, Elasto-adhesive models, Hertz, JKR, DMT, Sneddon

1 Introduction

AFM indentation is a widely used technique to probe the elastic properties of deformable materials, from synthetic or biological origin. This technique relies on indenting the material up to a certain force set point and then fitting the force-indentation curve with an appropriate rheological model. In case the elastic modulus is the main concern, the most common models to fit the curve are the Hertz or the Sneddon's models, depending on the geometry of the probe (spherical versus conical). These models assume a linear elastic response to indentation, the absence of viscosity, and the absence of adhesion between the AFM tip and the material. However, when indenting too strongly, materials undergo nonlinear elastic or plastic deformations [1, 2]. Identifying the elastic regime by eye on an indentation curve is far from obvious (Fig. 1). An efficient method consists in scaling the indentation curve to

Nuno C. Santos and Filomena A. Carvalho (eds.), *Atomic Force Microscopy: Methods and Protocols*, Methods in Molecular Biology, vol. 1886, https://doi.org/10.1007/978-1-4939-8894-5_16,

a)

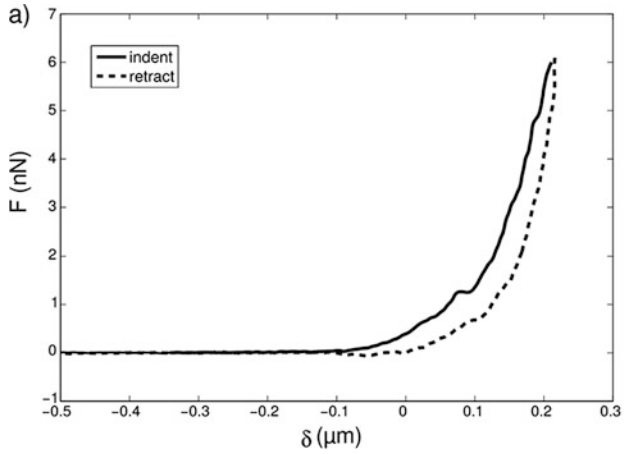

b)

Model \ Young's modulus (kPa)	Indent	Retract
Hertz	4.6	4.9
JKR	NA	4.2
DMT	NA	4.2

Fig. 1 (**a**) Example of experimental force-indentation curves with presumably low adhesion energy, obtained on a biological tissue using a spherical indenter of radius 5 μm. (**b**) Young's moduli obtained when fitting these curves. The fit on the indentation curve predicts a smaller Young's modulus than fits on the retract curve, due to the adhesion energy. Similarly, the fit using Hertz's model on the retract curve overestimates the Young's modulus, compared to JKR or DMT models, due to the adhesive force on the indenter

transform it to a linear curve [3]. For instance, Hertz's model predicts that the force opposed by a material against a spherical probe scales with the indentation as $F \propto \delta^{3/2}$, with F the loading force and δ the indentation depth. Then, plotting the indentation curve as $F^{2/3}(\delta)$ appears as a straight line if the material responds elastically. Identically, plotting $F^{1/2}(\delta)$ when indentation is performed with a conical or pyramidal tip allows identifying the range where the material deforms elastically.

This approach is valid as long as there is no adhesion between the tip and the material. But to first order, adhesion contributes with similar scaling laws to the deformation of the material when indentation is performed with a spherical probe [4]. Then, even if the material responds elastically to the indentation, the quantification of the Young's modulus is biased by the adhesive interaction that sucks the probe into the material: the Young's modulus is overestimated (Fig. 1). The aim of the present article is to propose a straightforward, easy-handling methodology to (i) identify the elastic regime and (ii) quantify the Young's modulus even in the presence of adhesion between the tip and the material.

2 Theory

2.1 Role of Adhesion in the Determination of the Young's Modulus for a Spherical Indenter

For a spherical indenter, in the absence of adhesive interaction between the indenter and the material and in the limit of linear elasticity, the force-indentation relationship is described by the Hertz's law [5]:

$$F_{\mathrm{n}} = KR^{1/2}\delta^{3/2} \tag{1}$$

with F_n the normal load, δ the indentation depth, R the radius of the indenter, and K the renormalized elastic modulus, related to the Young's modulus E and the Poisson's ratio ν of the material by the following formula: $K = 4E/3/(1-\nu^2)$.

In order to account for the adhesive interaction between the spherical probe and the material, we focus on two extreme regimes of adhesive interaction [6]: the Johnson-Kendall-Roberts (JKR) model and the Derjaguin-Muller-Toporov (DMT) model. JKR model applies for soft materials with large surface energies and probes with large radius of curvature. In this model, the adhesive interaction between the tip and the material dominates the elastic reaction force of the material. Then, at the point of contact, the probe is sucked by the material, which results in the deflection of the cantilever (Fig. 2). JKR model is described by the following set of equations [7]:

$$\delta = \frac{a_{JKR}{}^2}{R} - \frac{4}{3}\sqrt{\frac{a_{JKR}F_{ad}}{RK}} \tag{2}$$

$$a_{JKR} = \left(\frac{R}{K}\right)\left(\sqrt{F_{ad}} + \sqrt{F_n + F_{ad}}\right)^{2/3} \tag{3}$$

$$F_{ad} = \frac{3\pi}{2}\gamma R \tag{4}$$

with the same notations as in Eq. (1), γ is the adhesion energy (in N/m) and a_{JKR} the radius of the contact zone. On the other hand, DMT model applies for materials with low surface energy and probes with small radius of curvature. Here, adhesion enters as a perturbation to the elastic response of the material: the cantilever is not deflected at the point of contact. DMT model writes as [8]:

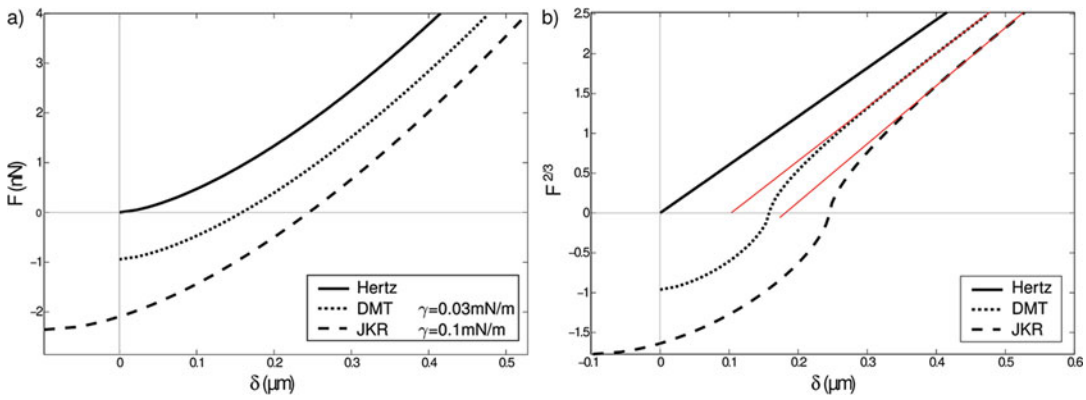

Fig. 2 JKR and DMT elasto-adhesive models can be approximated by the scaling law $F^{2/3}(\delta)$ on a significant range of indentation. a) Theoretical retract curves for a 4 kPa material with adhesion properties specified in the inset. (**b**) Plot of the same curves using the representation with the scaling law. The red lines are linear fits and delineate the elastic regimes

$$\delta = \left(\frac{F_n + F_{ad}}{KR^{1/2}}\right)^{2/3} \tag{5}$$

$$F_{ad} = 2\pi\gamma R \tag{6}$$

Both equations, Eqs. (2–4) and (5, 6), can be linearized. In the JKR model (Eqs. (2–4)), the loading force F_n that the cantilever measures mainly results from the adhesive interaction: $F_n \simeq F_{ad}$. On the contrary, in the DMT model, the loading force F_n mainly opposes the elastic resistance of the material: $F_n \gg F_{ad}$. Then, replacing F_{ad} by F_n in Eqs. (2 and 3) and neglecting F_{ad} in Eq. (5), both lead to zeroth order to the same scaling law:

$$F_n^{2/3} \sim \delta \tag{7}$$

This scaling law is identical to the scaling law that relates the loading force to the indentation depth in the case of a purely elastic interaction (Eq. 1), although in the JKR model F_n is dominated by the adhesive interaction and not by the elastic resistance to indentation. As shown in Fig. 2, the linearization of Eqs. (2–4) or Eqs. (5 and 6) is in practice valid on a significant range of the force-indentation curve. This approach then allows identifying the part of the force-indentation curve that can be safely fitted to extract the elasto-adhesive parameters, K and γ, of the material.

Once the relevant part of the force-indentation curve has been bracketed, an additional question raises, that is, the need of accounting of the adhesive interaction when indenting with a spherical probe. In particular, if the DMT model is appropriate to fit the force-indentation curve, could the Hertz's model be sufficient as the adhesive interaction only enters as a perturbation? As shown in Fig. 3, Hertz's model only keeps valid for very low

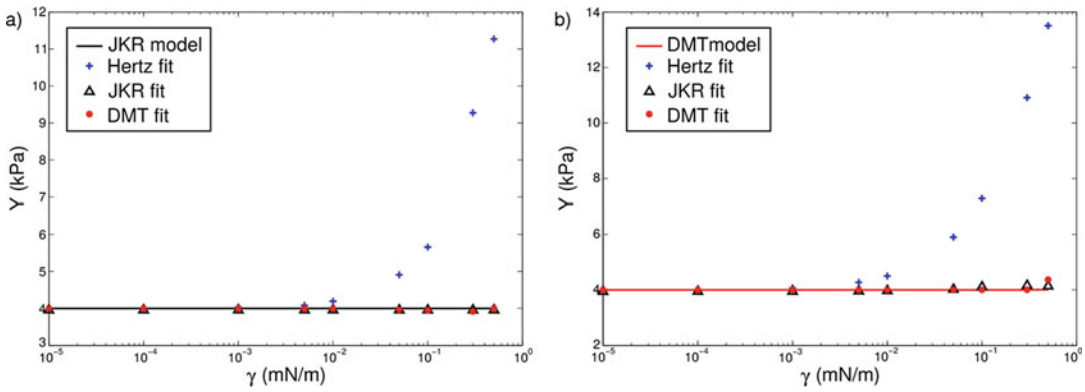

Fig. 3 In the presence of adhesion, Hertz's model overestimates the Young's modulus. JKR and DMT models give, however, similar result concerning the Young's modulus. (**a**) Hertz, JKR, and DMT fits were performed on a theoretical retract curve obtained by plotting JKR model for a panel of adhesive interactions ($Y = 4$ kPa). (**b**) Same as (**a**), based on a theoretical retract curve obtained using DMT model with the same Young's modulus ($Y = 4$ kPa)

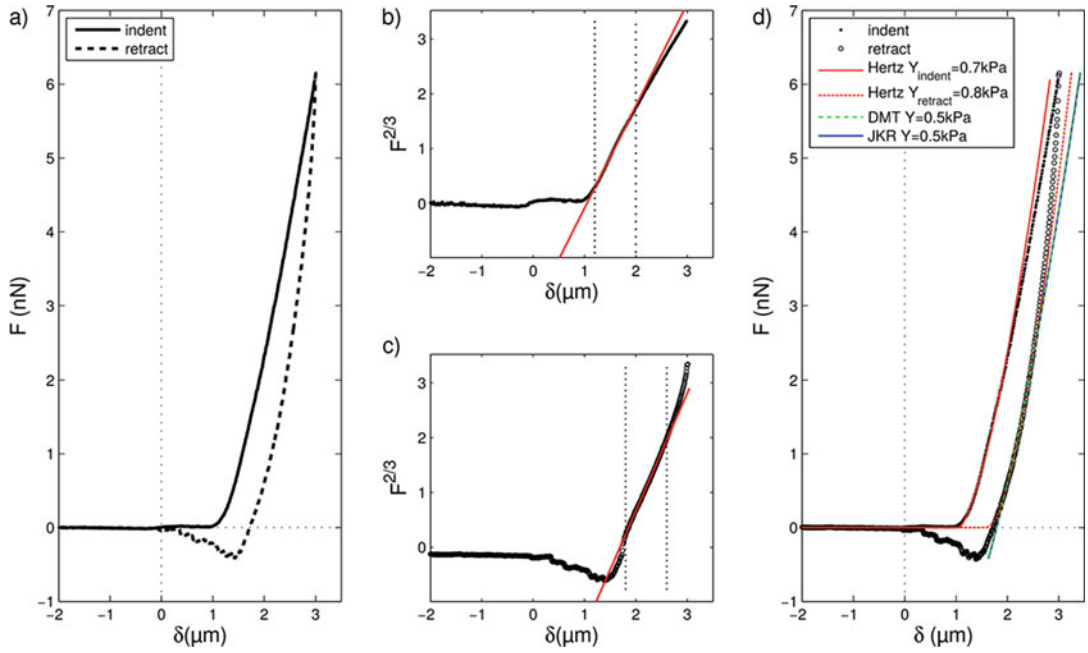

Fig. 4 Steps for fitting a force-indentation curve. (**a**) Experimental curves. (**b**, **c**) Plots of the indent (**b**) and retract (**c**) curves using the scaling law representation allows the delineation the elastic regime. Dotted lines mark out the boundaries of the linear regime. Red lines are linear fits performed in this range. (**d**) Fits using Hertz (red), DMT (green), and JKR (blue) models are performed in the elastic range

adhesion energy between the probe and the material. In general, fitting the retract curve with Hertz's model leads to overestimate the Young's modulus (Figs. 1 and 4), as expected as the probe is retained by the adhesive interaction into the material. More surprisingly, even in the presence of large adhesion, DMT and JKR models give similar results for the Young's modulus (at least within the error bar of the AFM measurement). Only the adhesion energy γ is noticeably influenced by the choice of the elasto-adhesive model. To conclude, it is safer to account for the adhesion energy when quantifying the elastic properties of the indented material. If a proper quantification of the adhesion energy is not required, then, as shown in Fig. 3, testing only one of the elasto-adhesive models, either DMT or JKR, is sufficient to quantify the Young's modulus of the material with no significant consequence on the statistical distribution [4].

2.2 Sharp Tips and the Contribution of the Adhesion Energy

The analog of the Hertz's model for a conical tip is the Sneddon's model [9]:

$$F_{\mathrm{n}} = \frac{3}{2\pi} K\delta^2 \tan\theta \tag{8}$$

K is still the renormalized Young's modulus, and θ is the half angle of the cone. Other formulas have been derived for more sophisticated geometries like pyramids (*see* [10], for example, for a listing of formula for other geometries). The precise geometry influences the prefactor in Eq. 8), but the scaling law is preserved. Then, the elastic regime in the force-indentation curve can be found by plotting ${F_n}^{1/2}(\delta)$.

In principle, the adhesion energy could also contribute to the deflection of the cantilever. However, the adhesion energy is proportional to the surface of contact. For similar indentation depths, indentation with a conical or a spherical indenter results in surfaces of contact with different order of magnitude. The ratio of the surfaces of contact is

$$\frac{A_{\text{sphere}}}{A_{\text{cone}}} = \frac{2R\cos\theta}{\delta\tan\theta} \tag{9}$$

with R the radius of the spherical probe, θ the half angle of the conical tip, and δ the indentation depth. For typical values such as a radius of 5 μm, an angle of 18°, and an indentation depth of 0.5 μm, $A_{\text{sphere}}/A_{\text{cone}} \simeq 58$. Then, as the surface of contact is much smaller for a conical or a pyramidal tip, the adhesion energy is also much smaller, and, in general, it can be neglected.

In case adhesion would significantly influence the quantification of the Young's modulus, Sirghi et al. proposed a correction term to the Sneddon's theory for a conical tip (analog to DMT theory) [11]:

$$F_n = \frac{3K\tan\theta}{2\pi}\delta^2 - F_{ad} \tag{10}$$

$$F_{ad} = \frac{8\gamma\tan\theta}{\pi\cos\theta}\delta \tag{11}$$

or a pyramidal one [12]:

$$F_n = \frac{3K\tan\theta}{\pi^{3/2}}\delta^2 - F_{ad} \tag{12}$$

$$F_{ad} = \frac{32\gamma\tan\theta}{\pi^2\cos\theta}\delta \tag{13}$$

with the same notation as before. Here again, the loading force, F_n, is supposed to dominate the adhesion force, F_{ad}. Using the linearization technique to find the most relevant region of the force-indentation curve to fit the elastic parameters still holds.

The limit of large adhesion energy (analog to the JKR theory) has also been solved with modeling the indenter as a small sphere compared to the contact radius, or as a hyperboloid indenter [13]. For soft biological samples, the hyperboloid indenter is a more relevant model, as the indentation is larger than the radius

of the spherical cap of the sharp tip. We then only report this set of equations:

$$\delta = \frac{a}{2\tan\theta}\Psi - \left(\frac{F_{ad}}{RK}\right)^{1/2} \tag{14}$$

$$F_n = \frac{3K}{4\tan^2\theta}\left(aR + \frac{a^2\tan^2\theta - R^2}{2\tan\theta}\Psi\right) - \frac{3Ka}{2}\left(\frac{F_{ad}}{RK}\right)^{1/2} \tag{15}$$

$$F_{ad} = \frac{8\pi}{3}\gamma R \tag{16}$$

$$\Psi = \frac{\pi}{2} + \arcsin\left(\frac{a^2\tan^2\theta - R^2}{a^2\tan^2\theta + R^2}\right) \tag{17}$$

F_n, δ, K and γ keep the same notations as before. Specific to Eqs. (14–17), R is the radius of curvature of the apex of the tip, a is the contact radius, and θ is the half angle of aperture of the tip. As it can be seen in Eqs. (14–17), the limit $F_n \simeq F_{ad}$ does not lead to a linear relationship between the indentation, δ, and a power law of the load, F_n. In this specific case of large adhesion of a sharp tip, the proposed methodology to find the linear elastic or elasto-adhesive regime does not hold anymore. The sliding window technique [14] or an optimization method for fitting the curve [10] is then required.

In the next section, we illustrate the methodology to fit an experimental force-indentation curve obtained by indenting an immersed biological tissue with a spherical indenter [4]. This approach is easily adapted to the analysis of force-indentation curves obtained with a sharp tip with limited adhesion (Eqs. 10 and 11 or 12 and 13).

3 Methods

The following methodology addresses the analysis of force-indentation curves obtained with a spherical probe. The AFM must have been calibrated in sensitivity and stiffness. Indent and retract curves are acquired with identical velocities of the piezo (*see* **Note 1**). They are printed in the form $F_n(\delta)$.

1. Check the shift between the baselines of the indent and retract curves. A deviation larger than the shift that is observed during the calibration of the stiffness of the cantilever means that the sample undergoes plastic deformations. As long as this plastic deformation keeps much smaller than the range of the elastic regime, it can safely be neglected. Otherwise, an analysis based on linear elasticity is no more relevant.

The next steps of the analysis are performed on the retract curve, as analytical elasto-adhesive models tackle the unloading of the indenter.

2. Filtering of the data to remove noise: running average or Gaussian filter. This step is often proposed in processing software associated to AFM.
3. Alignment of the baseline: the baseline must be tilted and aligned with zero load. Also often proposed in AFM processing software.
4. Optional: positioning the zero depth at the crossing between the retract curve and the zero load (*see* **Note 2**).

   From this step, programing may be required, as most of the AFM processing software do not include the following steps.
5. Plot the data as ${F_n}^{2/3}(\delta)$ if the indenter is a sphere (or plot ${F_n}^{1/2}(\delta)$ if the indenter is a pyramid or a cone, *see* Theory).
6. Select the largest straight region of the plot as shown in Fig. 4c (*see* **Note 3**). The boundaries of the straight fit bracket the range where the elasto-adhesive model is to be fitted. This step can be performed either by hand, by superimposing a straight line on the plot and finding graphically the limit of the superimposition of the straight line with the scaled retract curve, or automatically, by fitting an increasing portion of the curve with a straight line and using a r-square criterion to find the limit of the linear regression (For example, $r^2 > 0.95$, meaning that less than 5% of the data escape the fit).
7. Fit the $F_n(\delta)$ data using Hertz, JKR, and/or DMT models, using Eqs. (1–6) with the following fitting parameters: (i) the Young's modulus (or equivalently K); (ii) the adhesion energy γ; and (iii) the contact point δ_0, which enters Eqs. (1, 2 and 5) by replacing δ by $\delta - \delta_0$ (*see* **Notes 4** and **5**).

4 Notes

1. The choice of the velocity of the piezo is a compromise between the gain of time and the perturbation of the measurement by the viscosity of the immersion liquid and/or the material. In order to be sure to get rid of viscous effects, change this parameter and check that the curves keep unchanged.
2. This handmade translation of the curve is useful for automation of the fits of multiple curves, as it will allow using a unique set of guess values for the fit. The fitting procedure will then be insensitive to the flatness of the material. However, if one wants to obtain topographic information from an indentation map, then this step should not be performed. The fitting parameter δ_0 (described in Subheading 3, **step 7**) will provide the relative

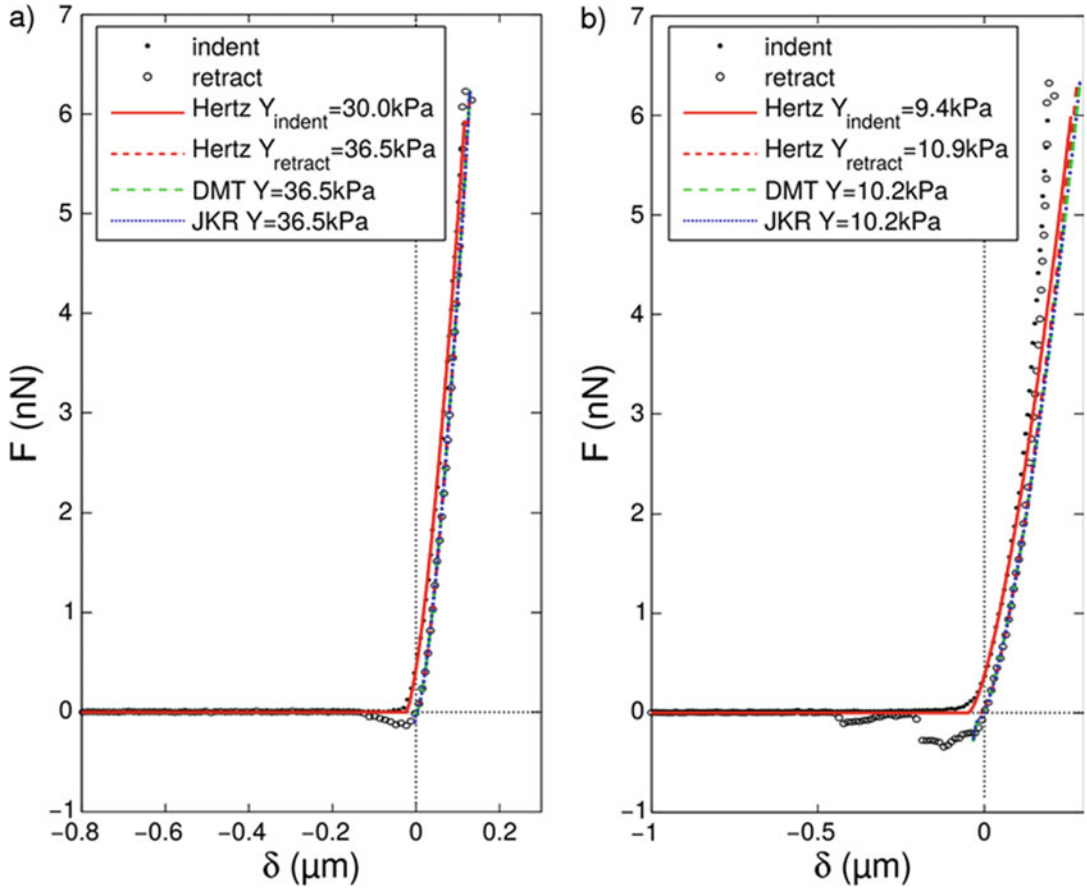

Fig. 5 (**a**) Example of a force-indentation curve where the Hertz's model correctly fits the retract curve. The retract curve keeps elastic on a wide range of force. (**b**) The precise shape of the adhesive interaction does not prevent from fitting with good accuracy the elasto-adhesive regime (*see* **Note 6**)

variation of height of the different indentation points scanned on the material.

3. The largest the linear region, the more robust the final fit to the initial guesses.
4. The degree of freedom on the contact point is critical for a good fit. When the linear region is properly defined, the fits appear fairly robust to the initial guesses of the fits.
5. Adhesion may be neglected when the interval of the force-indentation curve that is fitted is large enough to reach indentation depths that are far enough from the contact point (this distance depends on the strength of the adhesive interaction) (Fig. 5a). Hertz's fit converge to DMT or JKR fits if the interval of fit is far enough from the contact point.
6. The precise shape of the adhesive interaction does not prevent from getting precise fits. When the adhesion results in a retract

curve shaped very differently from JKR or DMT profiles (Fig. 2a), the adhesive region does not follow the scaling law presented in Eq. (7). The fit is performed out of this region. Consequently, only the part of the retract curve out of this rocky ride region is correctly fitted (Fig. 5b).

Acknowledgments

The authors acknowledge the support by ANR-12-JSVE05-0008. The authors are indebted to the AFM platform of the Interdisciplinary Laboratory of Physics, Grenoble, France, for their hosting.

References

1. Lin DC, Dimitriadis EK, Horkay F (2007) Elasticity of rubber-like materials measured by AFM nanoindentation. Express Polym Lett 1:576–584
2. Cappella B, Dietler G (1999) Force-distance curves by atomic force microscopy. Surf Sci Rep 34:1–104
3. Cappella B, Kaliappan SK, Sturm H (2005) Using AFM force-distance curves to study the glass-to-rubber transition of amorphous polymers and their elastic-plastic properties as a function of temperature. Macromolecules 38:1874–1881
4. Bouchonville N, Meyer M, Gaude C, Gay E, Ratel D, Nicolas A (2016) AFM mapping of the elastic properties of brain tissue reveals kPa/μm gradients of rigidity. Soft Matter 12:6232–6239
5. Lin DC, Dimitriadis EK, Horkay F (2007) Robust strategies for automated AFM force curve analysis—I Non-adhesive indentation of soft, inhomogeneous materials. J Biomech Eng 129:430–440
6. Lin DC, Dimitriadis EK, Horkay F (2007) Robust strategies for automated AFM force curve analysis—II: adhesion-influenced indentation of soft, elastic materials. J Biomech Eng 129:904–912
7. Johnson KL, Kendall K, Roberts AD (1971) Surface energy and the contact of elastic solids. Proc R Soc London Ser A 324:301–313
8. Derjaguin B, Muller V, Toporov Y (1975) Effect of contact deformations on the adhesion of particles. J Colloid Interface Sci 53:314–326
9. Oliver WC, Pharr GM (1992) An improved technique for determining hardness and elastic modulus using load and displacement sensing indentation experiments. J Mater Res 7:1564–1583
10. Lin DC, Horkay F (2008) Nanomechanics of polymer gels and biological tissues: a critical review of analytical approaches in the Hertzian regime and beyond. Soft Matter 4:669–682
11. Sirghi L, Rossi F (2006) Adhesion and elasticity in nanoscale indentation. Appl Phys Lett 89:243118–243118-3
12. Sirghi L, Ponti J, Broggi F, Rossi F (2008) Probing elasticity and adhesion of live cells by atomic force microscopy indentation. Eur Biophys J 37:935–945
13. Sun Y, Akhremitchev B, Walker GC (2004) Using the adhesive interaction between atomic force microscopy tips and polymer surfaces to measure the elastic modulus of compliant samples. Langmuir 20:5837–5845
14. Domke J, Radmacher M (1998) Measuring the elastic properties of thin polymer films with the atomic force microscope. Langmuir 14:3320–3325